

Dispersive Chaos in One-Dimensional Traveling-Wave Convection

Paul Kolodner, James A. Glazier, and Hugh Williams
AT&T Bell Laboratories, Murray Hill, New Jersey 07974-2070
 (Received 1 June 1990)

We report experiments on weakly nonlinear traveling-wave convection in an annular cell. The evolution of small-amplitude waves consists of the repetitive formation and sudden collapse of spatially localized pulses. This leads to continuously erratic dynamics with no stable saturated state, even near onset, and even when convection begins with a unidirectional, nearly spatially uniform state. Such behavior is reminiscent of simulations of the complex Ginzburg-Landau equation in the limit of strong nonlinear dispersion.

PACS numbers: 47.25.Qv, 47.20.Ky, 47.20.Tg

Convection in a thin, horizontal layer of a binary fluid mixture which is heated from below has emerged in recent years as an interesting nonequilibrium system for studying the physics of pattern formation. When the temperature difference applied across the layer exceeds a certain threshold, the quiescent state gives way to a state of traveling waves (TW). Above onset, a wide variety of nonlinear TW states can occur. For example, experiments in narrow rectangular cells¹ have revealed one-dimensional TW states in which wave energy “sloshes” or “blinks” back and forth across the cell. In this geometry, reflections from the end walls of the cell lead to the existence of two counterpropagating wave components, and Cross² has asserted that the saturating nonlinear interaction between them is responsible for the dynamical behavior. Numerical simulations of a model of this physics, consisting of a system of two coupled Ginzburg-Landau equations for the complex wave amplitudes (CGLE), with real coefficients, exhibit behavior which closely parallels the experimental results.²

In this paper, we report that, when the same experiments are repeated in an annular cell, in which there are no end-wall reflections, completely different dynamical behavior occurs. A small-amplitude, unidirectional wave train exhibits repeated episodes of linear growth, formation of a spatially localized pulse, and sudden collapse. This leads to a continuously erratic state arbitrarily close to onset, even if convection begins with a state of unidirectional TW. The measured parameters of the system are shown to correspond to a limit of strong nonlinear dispersion in the CGLE, and our observations bear a striking resemblance to numerical simulations³ of the CGLE in this limit. Thus we refer to this spatio-temporal behavior as “dispersive chaos.” We believe that our results constitute the first experimental observation of this kind of dynamical behavior.

We use an improved version of a previously described apparatus.⁴ The cell is an annular channel formed by a plastic disk and ring which are clamped between a rhodium-plated, mirror-polished copper bottom plate and a sapphire top plate. The cell dimensions are $d=0.301$

cm height $\times 1.73d$ radial width $\times 80.1d$ mean circumference. Cooling water circulates azimuthally over the top plate, and the bottom plate is heated electrically. The temperature difference applied across the fluid layer, ΔT , is typically 3.9 K and is regulated with a stability of ± 0.3 mk. We have taken extreme care to minimize and measure azimuthal nonuniformities in ΔT , the cell height, and the channel width, and to level and symmetrically insulate the cell. We use shadowgraphic visualization to record the pattern of the TW.^{4,5} The convection is always observed to be one dimensional, consisting of superpositions of waves which propagate azimuthally around the cell in opposite directions (here called “left” and “right”). A computer calculates the profiles of the left and right TW in real time by complex demodulation of the shadowgraph data.⁵ In addition, a photomultiplier samples the light intensity at one point in the shadowgraph image. We obtained most of our results using a 0.40-wt% solution of ethanol in water at a mean temperature of 27.0°C, for which the separation ratio $\psi = -0.021$, the Prandtl number $P = 6.22$, and the Lewis number $L = 0.009$.⁶ We also report results for fluids with $\psi = -0.041$, -0.050 , and -0.069 .

The experimental procedure is similar to that used in previous work.^{1,4,5} The applied temperature difference ΔT is increased in small steps until growing TW appear. The oscillation threshold and initial frequency are consistent with linear theory,^{4,7,8} and the properties of the TW are independent of amplitude for sufficiently small amplitude. We identify the linear onset $\varepsilon \equiv (\Delta T - \Delta T_c) / \Delta T_c = 0$ with the value ΔT_c at which the sum of the spatial averages of the demodulated left- and right-wave amplitudes exhibits a vanishing growth rate. By allowing the linear waves to grow to some small amplitude and then setting $\varepsilon = 0$, we can produce linear TW whose amplitudes are time dependent and spatially uniform to within a factor 2, with nonuniformities corresponding to a small, fixed spatial variation in ε .⁵ These states typically exhibit comparable left- and right-wave amplitudes. However, we can also prepare unidirectional TW merely by increasing ΔT slightly above ΔT_c —typically by

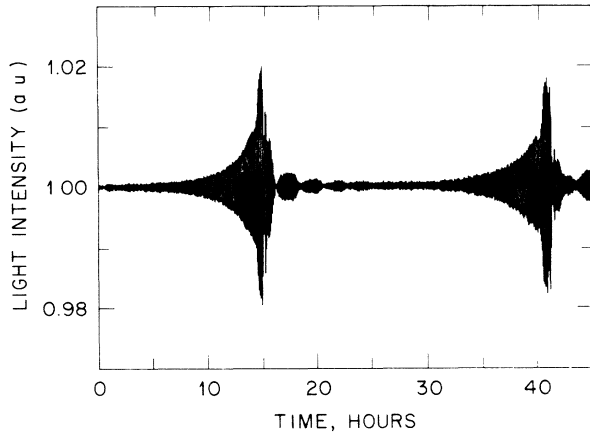


FIG. 1. The light intensity measured at one spatial point in the shadowgraph image as a function of time during the evolution of a unidirectional state at $\varepsilon=2.5 \times 10^{-4}$, for $\psi = -0.021$. The behavior consists of repeated linear growth and sudden pulsing, followed by an abrupt collapse to small amplitude. During this entire run, the left-going wave component remained at zero amplitude.

$\varepsilon=3 \times 10^{-4}$. At first, both TW grow in time with an amplitude-independent linear growth rate. Then, however, as predicted in Ref. 3, nonlinear effects cause one of the TW to decay. We can then reduce the amplitude of the remaining TW by briefly reducing ε below zero. This linear TW state remains unidirectional at least for times of the order of 1 day, indicating that reflections from imperfections in the apparatus are weak.

Once a unidirectional linear state has been characterized, we can raise ε above zero again and study its nonlinear evolution. We observe that the evolution of a unidirectional wave consists of repeated pulses in space and time. Figure 1 shows the light-intensity signal at one spatial point during this evolution, for $\psi = -0.021$. The gradual linear growth seen at the beginning gives way to a burst of amplitude, followed by a sudden collapse. This sequence then repeats irregularly. For no positive ε does the system ever find a stable, saturated nonlinear TW state.⁹ Similar results are obtained for $\psi = -0.041$ and -0.050 .

We illustrate the spatiotemporal character of this pulsing in Fig. 2. Initially, the state consists of small-amplitude waves traveling to the right at the linear phase velocity s_{lin} , with a fairly uniform spatial amplitude profile. As the wave amplitude grows, the system forms a spatially localized pulse which fills from one-tenth to one-half of the cell, depending on parameters. The propagation velocity drops abruptly at some point during the formation of this pulse to a new value $s_{\text{nonlin}} \leq s_{\text{lin}}/10$. After further growth and propagation at s_{nonlin} , the wave amplitude abruptly collapses, and the process repeats. The spatial location of subsequent pulses appears to be random. The nonlinear pulse velocity s_{nonlin} is approximately constant throughout the life of each pulse and

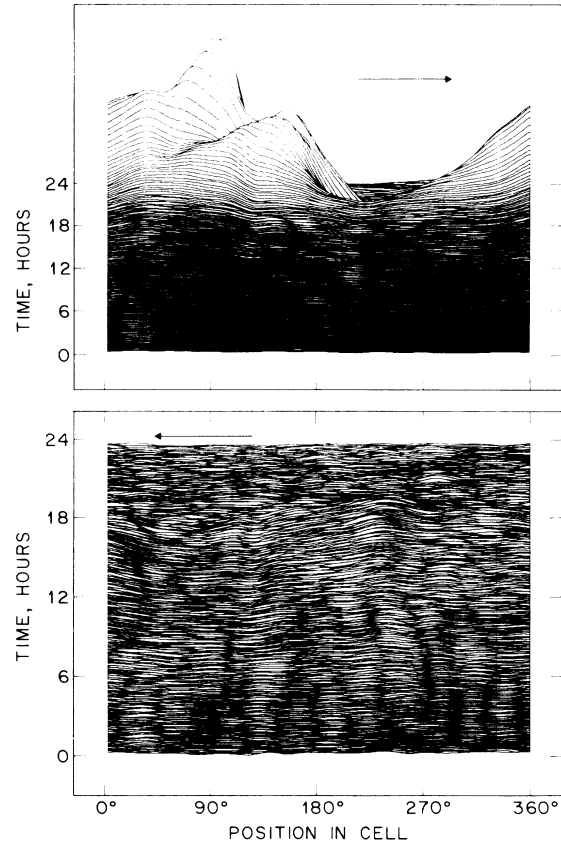


FIG. 2. Hidden-line plots showing the spatiotemporal behavior of the right-going (top) and left-going (bottom) wave-amplitude profiles at $\varepsilon=1.8 \times 10^{-4}$, during a run with $\psi = -0.021$. The traces in these plots show the wave amplitude as a function of position at subsequent times, with time proceeding upwards. An initial, nearly uniform small-amplitude state of linear waves grows up into a double-humped spatial pulse which fills about half of the cell. This pulse will collapse everywhere in space and then grow up again. The left-going wave component remained at zero amplitude during this run.

has approximately the same value for different pulses.

This pulsing behavior occurs over a range of ε and ψ . If we begin with a unidirectional state, wave energy must gradually appear in the oppositely propagating component, on a time scale of about 10 pulse cycles. Alternatively, we may start with a state which contains similar energy in both components. In either case, the pulse behavior described above appears to occur independently in the individual wave components. This is illustrated in Fig. 3, which also shows that the density of pulses in time and space increases with ε .

We have seen similar spatiotemporal pulsing at $\psi = -0.021$, -0.041 , and -0.050 . As ψ is decreased from -0.021 to -0.050 , the average value of $s_{\text{nonlin}}/s_{\text{lin}}$ at $\varepsilon=0$ remains constant at 0.08, while the average temporal duration τ_p of the pulses decreases from 33 ± 5 to 12 ± 3 (measured in units of the vertical thermal

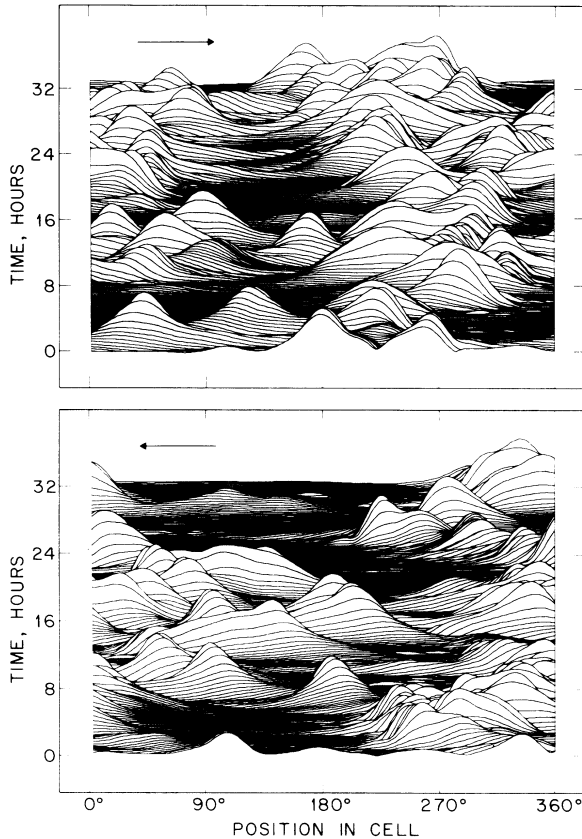


FIG. 3. Spatiotemporal behavior of the right (top) and left (bottom) wave components during a run at $\varepsilon = 5.6 \times 10^{-3}$, with $\psi = -0.021$. Both wave components exhibit a profusion of strongly localized pulses, and the evolutions of the two components appear to be independent. Note, in comparison with Fig. 2, that the density of pulses in space and in time is greater and that the spatial extent of the pulses is smaller at larger values of ε .

diffusion time). For $\psi = -0.069$, however, the behavior is completely different. The first pulse seen at $\varepsilon > 0$ evolves into a strongly localized, *stationary* confined state—i.e., $s_{\text{nonlin}} = 0$ and $\tau_p = \infty$. This agrees with recent observations at $\psi = -0.09$ and -0.08 by Niemela, Ahlers, and Cannell and Anderson and Behringer,¹⁰ but it is quite puzzling, since both s_{nonlin} and τ_p take values at this ψ which do not match extrapolations in ψ from the other data.

We can understand our observation of nonlinear pulsing of unidirectional TW in the context of the dispersive limit of the CGLE. With suitable scaling, this equation can be written to lowest order as follows:¹¹

$$\frac{\partial A}{\partial t} + s \frac{\partial A}{\partial x} = A + (1 + ic_1) \frac{\partial^2 A}{\partial x^2} - g(1 + ic_2) |A|^2 A. \quad (1)$$

Here, A is the amplitude of a right-going wave with group velocity s , c_1 is the linear dispersion coefficient, c_2 is the nonlinear frequency-renormalization coefficient, and $g = \pm 1$ is a saturation parameter. For TW convec-

tion, all the linear parameters in Eq. (1) are well known, on the basis of both theory⁷ and experiment.⁸ In particular, $c_1 = 0.022$ (-0.015 , -0.028) for $\psi = -0.021$ (-0.041 , -0.050). In general, other nonlinear terms must be added to Eq. (1) in order to properly model this physical system. For example, $g = -1$ for TW convection,^{1,12} so that a higher-order nonlinear term with a positive coefficient would be required to explain a saturated nonlinear state. Furthermore, in order to correctly model states of counterpropagating TW, one must write a corresponding CGLE for a left-wave amplitude B , with $s \rightarrow -s$, and one must include in both equations coupling terms like $|A|^2 B$ and $|B|^2 A$ to account for the interactions between the two waves. However, the observation that oppositely propagating wave components evolve independently means that these nonlinear coupling terms are small and are not the cause of the dynamical behavior we observe. Modulational instability¹³ can also be eliminated as the cause of this behavior. This instability is only important for saturated nonlinear waves, which are not seen in our experiments.

The key to understanding our observations lies in the observation that the nonlinear frequency-renormalization coefficient c_2 has a very large magnitude. We can make a measurement of c_2 by creating a unidirectional state of linear TW, raising ε above zero, and observing the development of its growth rate and frequency at low amplitudes, before any pulsing behavior occurs. Initially after such a jump in ε , the wave exhibits linear growth in its spatially averaged amplitude $\langle A \rangle$ with no obvious modification of the spatial profile. Once $\langle A \rangle$ becomes sufficiently large, however, we observe that the growth rate γ and the oscillation frequency Ω begin to deviate from the linear values by amounts $\delta\gamma, \delta\Omega \propto \langle A \rangle^2$. If we substitute a solution $\exp[(\gamma + i\Omega)t]$ into Eq. (1), we easily calculate $\delta\gamma = -g\langle A \rangle^2$ and $\delta\Omega = -gc_2\langle A \rangle^2$. Thus, our measurements of $\delta\Omega$ and $\delta\gamma$ give $c_2 = \delta\Omega/\delta\gamma = -7.2 \pm 1.2$ for $\psi = -0.021$. This is comparable to the value $c_2 = -9.7$ calculated by Schöpf¹² for this fluid.¹⁴

The observation that c_2 has a very large magnitude suggests that nonlinear dispersion is the cause of our pulsing behavior. We come to this conclusion by observing that, for the parameters of our experiments, Eq. (1) can be transformed into a dispersive form which has been found numerically to exhibit similar behavior.^{3,12} Since pulsing is observed for unidirectional TW, we can transform Eq. (1) into a comoving frame, in which the second term on the left-hand side vanishes. Because $c_2 \ll -1$, we can approximate the coefficient of the nonlinear term as ic_2 . Finally, because we observe similar behavior for both positive and negative c_1 , its sign is irrelevant. Thus, changing the sign of c_1 and taking the complex conjugate of Eq. (1), we arrive at the equation that was studied by Bretherton and Spiegel.³ These authors observed a pulsing behavior for $c_1 \gtrsim 0$ which bears a strong resemblance to our experimental observations

(cf. Fig. 3b of Ref. 3). They also gave a qualitative explanation for this pulsing: Because the nonlinear term in the CGLE is almost entirely imaginary, it acts only to damp the waves in regions of strong spatial gradients. This damping causes the edges of a spatial nonuniformity to steepen and contract, while its peak grows linearly, almost without saturation. Nonlinear dispersion, rather than saturation or modulational instability, dominates the dynamics.

The reason why erratic pulsing does not occur for $\psi \lesssim -0.05$ is that the nonlinear frequency-renormalization coefficient c_2 decreases in magnitude as ψ is decreased.¹² Thus, for sufficiently negative ψ , nonlinear dispersion ceases to dominate the dynamics, and some other mechanism takes over to stabilize motionless confined states. The reason why erratic pulsing does not occur in a rectangular cell for the same fluid parameters for which it is seen in annulus may be that the loss upon reflection of the TW from the end walls of the cell damps the growth of pulses. One might model this damping by increasing the real part of the nonlinear coefficient in the CGLE. In this case, the imaginary part of the nonlinear term will not be as important in the dynamics as its real part or the real parts of cross terms due to the presence of the other wave component. This puts the CGLE back in the "saturating" limit studied in Ref. 2.

To summarize, experiments on one-dimensional TW convection in an annular cell have revealed a new kind of spatiotemporal behavior which is characterized by the repetitive formation and sudden collapse of spatially localized pulses. Strong nonlinear dispersion appears to be the cause of this behavior.

We are pleased to acknowledge discussions with W. van Saarloos, B. I. Shraiman, H. Chaté, M. C. Cross, C. M. Surko, W. Schöpf, L. Kramer, and especially P. C. Hohenberg.

¹P. Kolodner, C. M. Surko, and H. Williams, *Physica* (Amsterdam) **37D**, 319 (1989); V. Steinberg, J. Fineberg, E. Moses, and I. Rehberg, *Physica* (Amsterdam) **37D**, 359 (1989).

²M. C. Cross, *Phys. Rev. A* **38**, 3593 (1988).

³C. S. Bretherton and E. A. Spiegel, *Phys. Lett.* **96A**, 152 (1983).

⁴P. Kolodner, D. Bensimon, and C. M. Surko, *Phys. Rev. Lett.* **60**, 1723 (1988); D. Bensimon, P. Kolodner, C. M. Surko, H. Williams, and V. Croquette, *J. Fluid Mech.* **217**, 441 (1990).

⁵P. Kolodner and H. Williams, in *Proceedings of the NATO Advanced Research Workshop on Nonlinear Evolution of Spatial-temporal Structures in Dissipative Systems*, edited by F. H. Busse and L. Kramer, NATO Advanced Study Institutes, Ser. B2, Vol. 225 (Plenum, New York, 1990), p. 73.

⁶P. Kolodner, H. Williams, and C. Moe, *J. Chem. Phys.* **88**, 6512 (1988).

⁷M. C. Cross and K. Kim, *Phys. Rev. A* **37**, 3909 (1988).

⁸P. Kolodner, C. M. Surko, and M. C. Cross (unpublished).

⁹This pulsing behavior is seen for $1.2 \times 10^{-4} < \varepsilon \lesssim 0.01$. Above this range, the cell fills with steady rolls via what appears to be the same convective-absolute transition seen in Ref. 1 at similar values of ψ in rectangular cells.

¹⁰J. J. Niemela, G. Ahlers, and D. S. Cannell, *Phys. Rev. Lett.* **64**, 1365 (1990); K. E. Anderson and R. P. Behringer, *Phys. Lett. A* **145**, 323 (1990).

¹¹A. C. Newell, in *Nonlinear Wave Motion*, edited by A. C. Newell, Lectures in Applied Mathematics Vol. 15 (American Mathematical Society, Providence, 1974), p. 157.

¹²W. Schöpf (private communication); W. Schöpf and W. Zimmerman, *Europhys. Lett.* **8**, 41 (1989).

¹³T. B. Benjamin and J. E. Feir, *J. Fluid Mech.* **27**, 417 (1967); J. T. Stuart and R. C. DiPrima, *Proc. Roy. Soc. London A* **362**, 27 (1978).

¹⁴A measurement of c_2 for a related TW system has been presented by V. Croquette and H. Williams, *Phys. Rev. A* **39**, 2765 (1989).

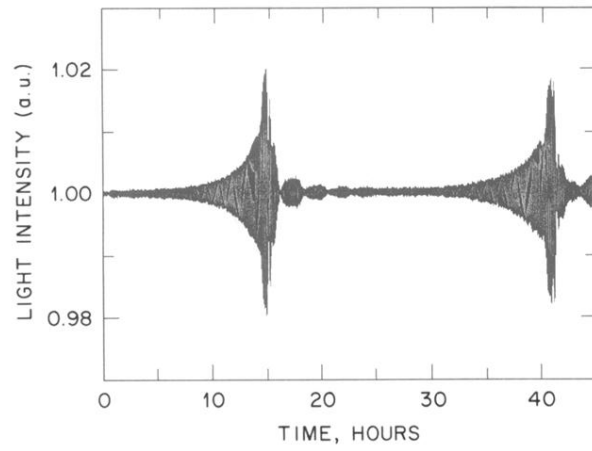


FIG. 1. The light intensity measured at one spatial point in the shadowgraph image as a function of time during the evolution of a unidirectional state at $\varepsilon=2.5\times 10^{-4}$, for $\psi=-0.021$. The behavior consists of repeated linear growth and sudden pulsing, followed by an abrupt collapse to small amplitude. During this entire run, the left-going wave component remained at zero amplitude.

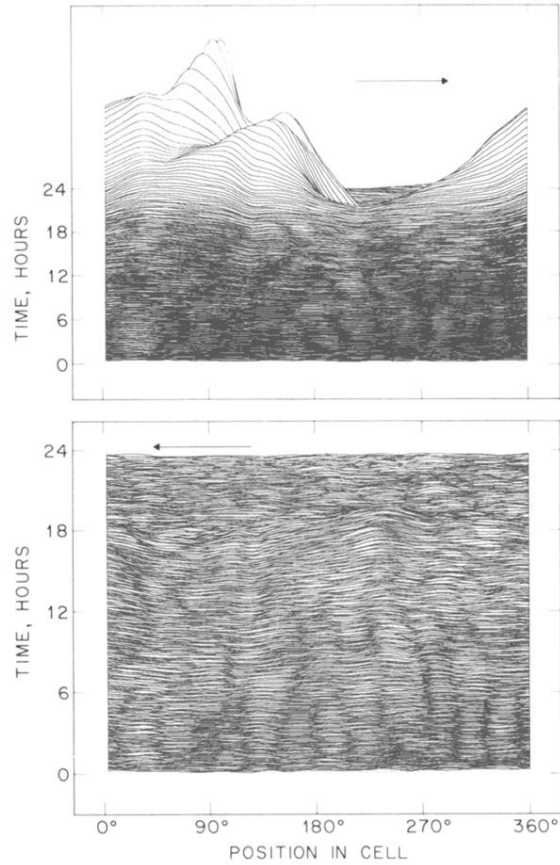


FIG. 2. Hidden-line plots showing the spatiotemporal behavior of the right-going (top) and left-going (bottom) wave-amplitude profiles at $\epsilon=1.8 \times 10^{-4}$, during a run with $\psi = -0.021$. The traces in these plots show the wave amplitude as a function of position at subsequent times, with time proceeding upwards. An initial, nearly uniform small-amplitude state of linear waves grows up into a double-humped spatial pulse which fills about half of the cell. This pulse will collapse everywhere in space and then grow up again. The left-going wave component remained at zero amplitude during this run.

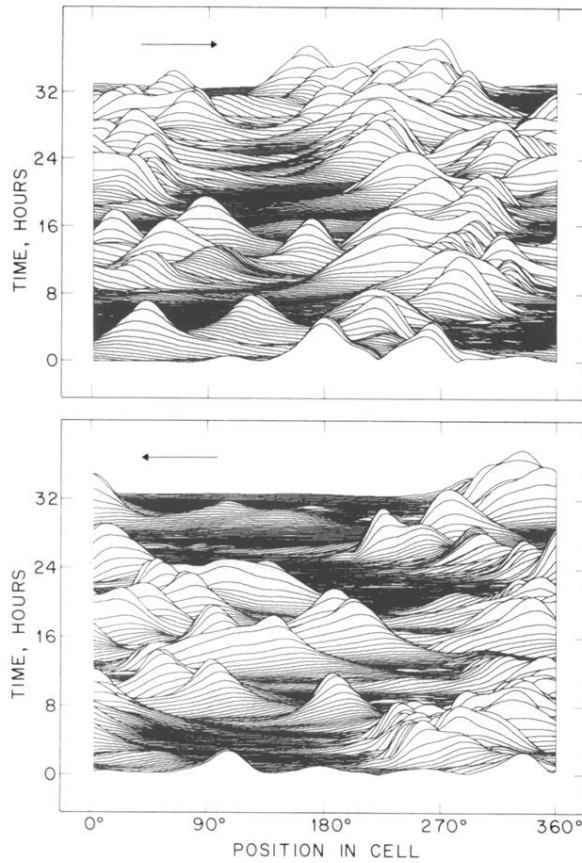


FIG. 3. Spatiotemporal behavior of the right (top) and left (bottom) wave components during a run at $\varepsilon = 5.6 \times 10^{-3}$, with $\psi = -0.021$. Both wave components exhibit a profusion of strongly localized pulses, and the evolutions of the two components appear to be independent. Note, in comparison with Fig. 2, that the density of pulses in space and in time is greater and that the spatial extent of the pulses is smaller at larger values of ε .